

Dynamics and Stability of Resistive Wall Mode in the JT-60U High- β Plasmas

G. Matsunaga, Y. Sakamoto, N. Aiba, K. Shinohara, M. Takechi, T. Suzuki, T. Fujita, A. Isayama, N. Oyama, N. Asakura, Y. Kamada, T. Ozeki and the JT-60 team
 Japan Atomic Energy Agency, Naka 311-0193, Japan
 E-mail: matsunaga.go@jaea.go.jp

Abstract. The dynamics and stability of the resistive wall mode (RWM) are investigated in the JT-60U high- β plasmas, and the sustainment of high- β plasmas above the ideal no-wall β -limit $\beta_N^{\text{no-wall}}$ has been demonstrated using a plasma rotation. To suppress an $n = 1$ RWM that limits the achievable β_N in the regime $\beta_N > \beta_N^{\text{no-wall}}$, the plasma rotation is kept larger than the critical rotation. Therefore, we have successfully sustained $\beta_N \simeq 3.0$ for ~ 1 s or $\beta_N \simeq 2.8$ for ~ 5 s. In this high- β_N regime, the MHD instabilities relating the RWM, that is, an $n = 1$ bursting mode and a slowly growing mode, have been observed. These modes sometimes induce the plasmas rotation damping and triggering the RWM. Especially, the slowly growing mode can reduce the rotational shear around the $q = 2$ surface and finally trigger the RWM. These results shows the rotational shear at the rational surface is also important to determine the RWM stability as well as the plasma rotation speed. Moreover, the plasma rotation braking owing to the RWM have been observed. It is found that the RWM distortion can clearly induce the plasma rotation braking inside the $q = 2$ surface.

1. Introduction

For a future fusion reactor with an economical attractiveness, the operation on the high- β_N region is desirable because the fusion output is proportional to the square of β_N . Here, β_N is the so-called normalized beta defined as $\beta_N \propto \langle p \rangle / (B_T I_p)$, where $\langle p \rangle$, B_T and I_p are the volume-averaged pressure, plasma current and the toroidal magnetic field, respectively. However, the β_N -value is limited at the regime $\beta_N^{\text{no-wall}} < \beta_N < \beta_N^{\text{ideal-wall}}$ due to the resistive wall mode (RWM), where $\beta_N^{\text{no-wall}}$ and $\beta_N^{\text{ideal-wall}}$ are the ideal β -limits with no-wall and with an ideal wall that is a perfectly conducting wall. The RWM is an MHD instability that grows with the resistive wall time τ_w , which is about several millisecond on JT-60U vacuum vessel. Therefore, the stabilization of resistive wall mode (RWM) is one of the key issues for future fusion reactors. The MHD theories taking into account the plasma rotation and the wall resistivity predicted that the RWM is stabilized by the plasma rotation [1]. Moreover, recent experiments [2, 3] have shown the plasma rotation required for the RWM stabilizing is less than about 1% of Alfvén speed at the rational surface. However, the mechanism for the RWM stabilizing and the detailed dynamics, in particular, just before and during the RWM, are still not unclear. Therefore, we have carried out the experiments so as to clarify these points in the JT-60U high- β plasmas. In this paper, firstly, the result of demonstration of the high- β sustainment with suppressing the RWM by the plasma rotation is shown. Secondly, we have described the other MHD instabilities relating the RWM, that are the $n = 1$ bursting mode and the slowly growing mode. Additionally, the observed plasma rotation braking due to the RWM is shown.

2. Sustainment of high- β_N plasma above the no-wall ideal β -limit

A sustainment of the β_N is required for fusion reactor with an economical attractiveness. In the high- β_N above $\beta_N^{\text{no-wall}}$, the achievable β_N is limited by a low- n instability such as a RWM. On JT-60U, we have previously achieved to the high- β_N plasma up to $\beta_N \sim 4$, but it was not stationary but transiently. Figure 1(a) shows the achieved β_N versus the sustained time duration on JT-60U. In this experimental campaign, we have tried to sustain high- β_N plasma with suppressing the RWM by the plasma rotation. In the consequence, $\beta_N \simeq 3.0$ for ~ 1 s or $\beta_N \simeq 2.8$ for ~ 5 s have been successfully sustained. However, at almost all discharges on the

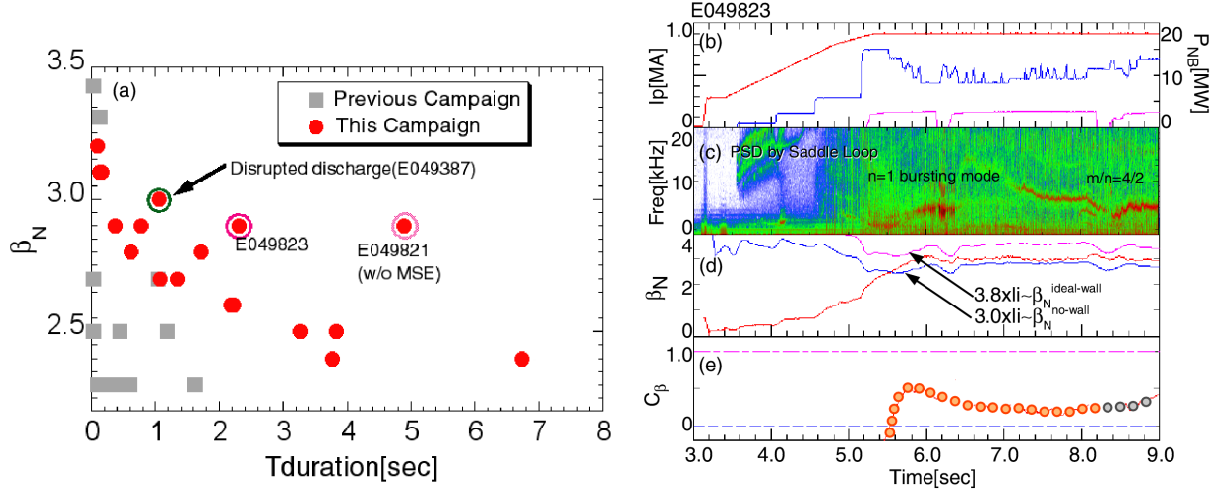


Fig. 1: (a) Achieved regime for time duration and β_N for high- β_N operation on JT-60U. Waveforms of example discharge sustained for a few seconds: (a) Plasma current and NB injection powers, (b) power spectrum for magnetic fluctuation by saddle loop (c) temporal evolution of β_N , $3.0 I_i \sim \beta_N^{\text{no-wall}}$, $3.8 I_i \sim \beta_N^{\text{ideal-wall}}$ and (d) C_β .

high- β_N regime, some MHD instabilities that can induce the disruption have been observed. The details regarding these are shown and discussed at the below sections. An example discharge where the high- β_N value was stationary sustained is shown in Fig. 1(a). We have successfully sustained $\beta_N \simeq 2.8$ above $\beta_N^{\text{no-wall}}$. The duration is about 2 s that is the order of plasma current diffusion time $\tau_R \sim 1$ s in this plasma. The waveforms of this discharge is shown in Fig. 1(b)-(e). In this discharge, in order to suppress the RWM that could limit the β_N -limit in this β_N -region, the plasma rotation was kept above the critical rotation ~ 20 km/s by the tangential NB injection. Particularly, a further rotation in the co-direction was kept by the tangential co-NBs. To estimate q -profile, one of the ctr-NBs was injected from 7.0 s, in turn, the toroidal rotation decreased. From the MARG2D which is the ideal MHD stability code [4], the β_N -limit with no-wall $\beta_N^{\text{no-wall}}$ is ~ 2.6 , which can be roughly indicated as $3.0 I_i$. While the ideal wall limit $\beta_N^{\text{ideal-wall}}$ is 3.2, which is roughly described as $3.8 I_i$. Therefore, the $C_\beta \simeq 0.3 > 0$ was sustained for about 2 s until an appearance of $m/n = 4/2$ island, which may be a neoclassical tearing mode (NTM). Here, C_β is an indicator that show how much the $\beta_N^{\text{no-wall}}$ is exceeding $\beta_N^{\text{no-wall}}$ defined as $C_\beta = (\beta_N - \beta_N^{\text{no-wall}}) / (\beta_N^{\text{ideal-wall}} - \beta_N^{\text{no-wall}})$. The ideal MHD stability analysis only makes sense without any resistive instability such as the $m/n = 4/2$ NTM.

3. Observation of disruptive MHD instabilities on $\beta_N > \beta_N^{\text{no-wall}}$

As mentioned above, almost discharge on these high- β_N plasmas, disruptive MHD instabilities appeared and then the discharge was terminated. Figure 2 shows an example discharge where several MHD instabilities continued to appear. Note that on this discharge, C_β was achieved about 0.8. At high- $\beta_N > \beta_N^{\text{no-wall}}$, an $n = 1$ bursts frequently appeared. The $n = 1$ bursts have the frequency chirping down and sometimes triggered the ELMs. After those, an instability was slowly glowing, of which growth time is $\tau_g \simeq 50$ ms. This slowly glowing mode gradually changed the plasma rotation profile, in particular, the rotational shear at $q = 2$ surface. It should be noted that these can be only observed in the high- β_N plasmas above $\beta_N^{\text{no-wall}}$. After that, the $n = 1$ RWM was growing with the wall time scale τ_w , finally, the discharge was disrupted.

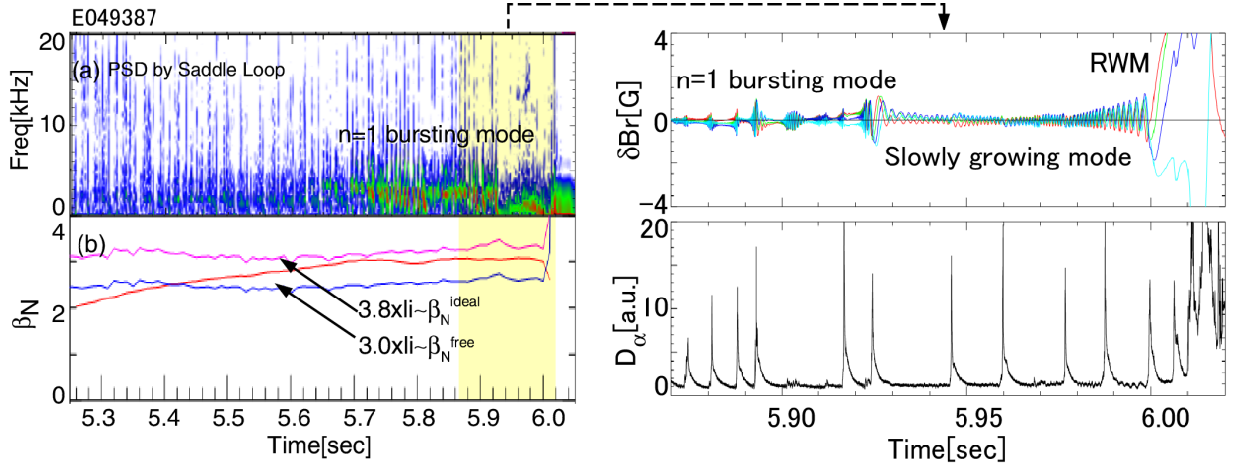


Fig. 2: Waveforms of example discharge with some MHD instabilities before the RWM onset. (a) Power spectrum for magnetic fluctuation by saddle loop (b) temporal evolution of β_N , $3.0I_1 \sim \beta_N^{\text{no-wall}}$ and $3.8I_1 \sim \beta_N^{\text{ideal-wall}}$. And expanded waveforms, temporal evolutions of (c) $n = 1$ magnetic deviation and (d) D_α emission.

3-1. Features of $n = 1$ bursting mode

On these high- β_N plasmas, a bursting mode that has a very large amplitude up to 1 Gauss has been frequently observed. This mode has been only observed on the high- β_N above $\beta_N^{\text{no-wall}}$. The bursting mode sometimes directly induces the RWM onset despite the plasma rotation larger than a critical rotation for RWM stabilization. Also, this bursting mode can change to the slowly growing mode as is mentioned below. The growth and decay time of the bursting mode are a few milliseconds that is very similar to the RWM growth time τ_w . Figure 3(a) and (b) show the typical waveform of the bursting mode with the time evolution of the mode frequency and D_α emission, and q -profile at $t = 5.90$ s. The toroidal mode number of this bursting mode is clearly $n = 1$, while the poloidal one seems to be $m = 3 \sim 4$. It should be noted that the amplitude of this mode at the low-field side (LFS) is much larger than one at the high-field side (HFS), thus, it is a ballooning structure. This mode is sometimes, but not always, synchronized with the D_α spikes probably due to the ELMs. Figure 4 shows a contour plot of the electron temperature T_e in the range $0.1 \leq \rho \leq 0.8$ by the ECE measurement and the $n = 1$ magnetic field deviation by the saddle loops. Also, the T_e fluctuation due to the bursting mode has been observed. The dashed line indicates the $q = 2$ surface by the MSE measurement. As shown in Figure 4(a), the T_e fluctuation due to the bursting mode does not behave like a tearing mode

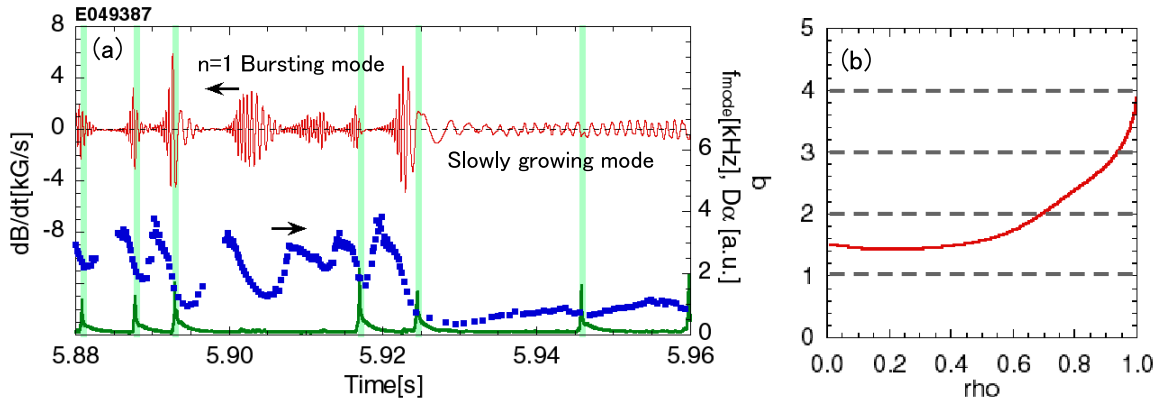


Fig. 3: (a) Amplitude of $n = 1$ bursting mode with the mode frequency and D_α emission. Vertical lines describe the ELM timings. (b) q -profile at $t = 5.90$ s

with a magnetic island. Rather, it is a global structure and spreads with the peak around $q = 2$ surface.

The initial mode frequency of this bursting mode is $f_{\text{burst}} \simeq 4$ kHz. The mode frequency repeats to chirp down as the amplitude was increasing. The bursting mode rotates in the co-direction toroidally and in the ion diamagnetic ω_*^i direction poloidally. To investigate the property of the mode rotation, plasma rotation at the $q = 2$ surface was changed from co- to ctr-direction. However, the direction of the mode rotation was always in the co-direction toroidally and in the ion diamagnetic ω_*^i direction poloidally. This means that the mode frequency can be independent of the toroidal rotation. At the present, it is not clear but the rotation

frequency is also similar to the precession frequency ω_{pr} of the trapped particle from the perpendicular neutral beams with the beam energy $E_b \simeq 90$ keV, thus, $f_{\text{pr}} = \omega_{\text{pr}}/(2\pi) \simeq 4$ kHz at the $q = 2$ surface. While the toroidal rotation and the ion diamagnetic drift frequency at the $q = 2$ surface are $f_{\text{tor}} \simeq 1$ kHz and $f_*^i = \omega_*^i/(2\pi) \simeq 1$ kHz, respectively

This mode is similar to waveform of the so-called fishbone mode associated with an $m/n = 1/1$ internal kink. However, as shown in Fig. 3(b), the center of safety factor q_0 is not close to unity. This means that this bursting mode is obviously different from an $m/n = 1/1$ fishbone instability because an $m/n = 1/1$ internal kink is fairly stable at this equilibrium. On the other hand, since the high- β_N is exceeding $\beta_N^{\text{no-wall}}$, the RWM is thought to be marginal. We speculate that this bursting mode is the mode that is destabilized by a resonance between a marginal RWM and a precession motion of energetic particles. To investigate the dependence of the beam pressure of the trapped energetic particles on the bursting mode stability, the NB power of the perpendicular units was scanned with keeping β_N . In consequence, the amplitude of the bursting mode is tend to reduce as the perpendicular NB power is reducing. Moreover, the growth time of the bursting mode is of order of the resistive wall time scale τ_w . Thus, this suggests that the bursting mode is one of the energetic particle driven modes (EPMs) and the results of a kinetic contribution of energetic particles to the RWM, that is, this can be called as "kinetic-RWM".

3-2. Observation of slowly growing mode

We have sometimes observed an $n = 1$ slowly growing mode just before the RWM onset as a RWM precursor in the range $\beta_N > \beta_N^{\text{no-wall}}$. This mode independently appears or is triggered by the bursting mode. As shown in Fig. 5, the β_N was not degraded during the slowly growing mode. This means that this mode does not directory affect the plasma confinement. Finally,

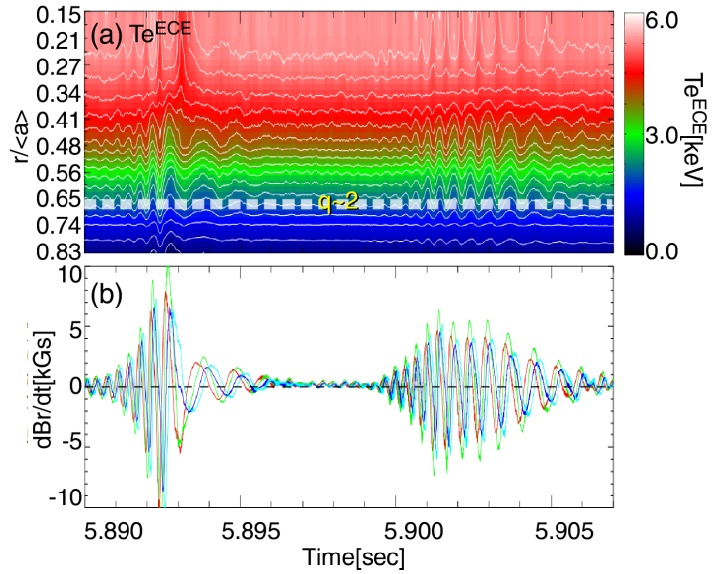


Fig. 4: (a) Contour plot of T_e by ECE measurement. Dashed line shows the $q = 2$ surface by MSE measurement. (b) $n = 1$ magnetic derivation by saddle loops. Different colors correspond to the saddle loops at the different toroidal locations.

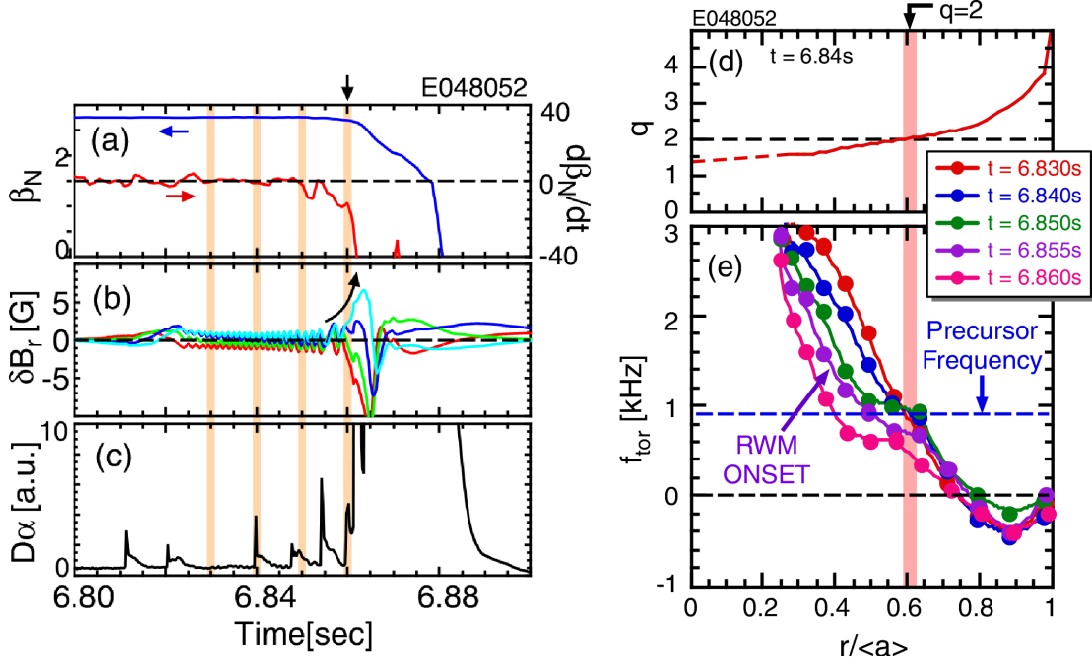


Fig. 5: Waveforms of example discharge with a slowly growing mode: (a) temporal evolution of β_N and $d\beta_N/dt$, (b) $n = 1$ magnetic deviation by saddle loops and (c) $D\alpha$ emission. (d) q and (e) toroidal rotation profiles with the precursor frequency.

this mode can induce the RWM onset, in turn, it leads to disruption. This mode has a growth time $\tau_g = 10 \sim 50$ ms that is longer than these of the RWM τ_w (the resistive wall time) and the ideal mode τ_A (the Alfvén time), and the real frequency corresponds to the plasma rotation at the $q = 2$ surface. Meanwhile, this growth time is similar to the growth time of the tearing mode $\tau_{\text{TM}} \sim \tau_R^{3/5} \tau_A^{2/5} \sim 50$ ms. However, the poloidal mode structure is similar to those of the above-mentioned $n = 1$ bursting mode, that is, a kink-ballooning mode-like structure, of which dominant poloidal component is $m = 3 \sim 4$ by the magnetic probes at the wall.

By the ECE measurement, the precursor does not have any island structures at the $q = 2$ surface. And rather, the amplitude at $q = 2$ surface seems to be dominant. These means that the radial structure is globally spread. For these reasons, the precursor is identified as neither NTM nor TM. The reason why this mode can induce the RWM onset is that this mode can reduce the rotation speed V_t and the rotational shear dV_t/dr around the $q = 2$ surface as shown in Fig. 5(e). The plasma rotation inside the $q = 2$ surface was decreasing as the mode was growing, while those outside the $q = 2$ surface was almost kept. Figure 6 shows the trajectories in the rotation speed V_t versus the rotational shear dV_t/dr at the $q = 2$ surface

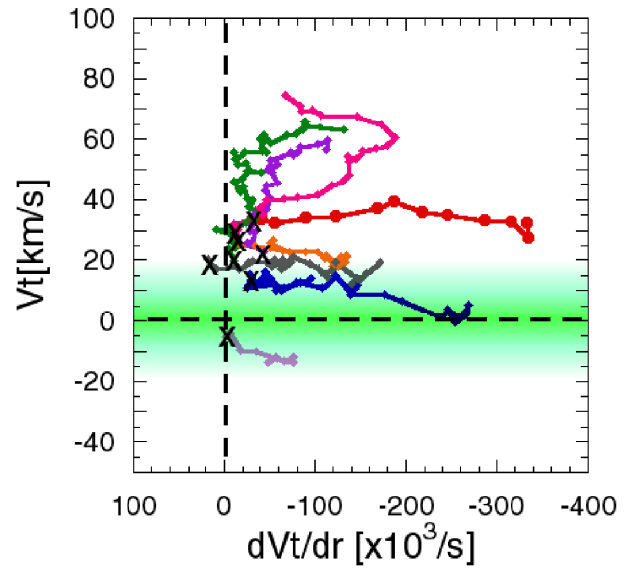


Fig. 6: Trajectories in the rotation speed V_t versus the rotational shear dV_t/dr at the $q = 2$ surface. "X"s stand for the RWM onsets.

during the slowly growing mode. The mark "X"s stand for the RWM onsets. The shadowed region indicates plasma rotation required for the RWM stabilization [2, 3]. Thus, it is predicted that the RWM becomes unstable if trajectory comes into this region. The line with full circles represents the trajectory of the above-mentioned discharge (E048052). On this trajectory, although the rotation speed was almost maintained, the rotational shear was monotonically decreasing. When the rotational shear was close to zero, the RWM was destabilized despite the enough rotation speed for the RWM stabilization. Note that, on some discharges, the above trajectories are getting across the shadowed region. This result suggests that the rotational shear around the rational surface is important to determine the RWM stability as well as the rotation speed. At the present, this precursor is thought to be essentially the same mode as the RWM and appears at the RWM stability boundary. The possible explanation for this slow growth time is that the kinetic effect of the trapped particle [5]. This effect is expected under the condition where the toroidal rotation is less than the ion diamagnetic frequency, thus, $f_{\text{tor}} \leq f_*^i$. As mentioned above, on these plasma, the plasma rotation is comparable to the ion diamagnetic frequency.

4. Plasma rotation braking due to RWM

The dynamics of the RWM in the growing phase is important because plasma rotation braking by the RWM itself could produce positive feedback for the RWM destabilizing. We have successfully measured the time evolution of plasma rotation profile in the RWM growing phase by using the fast CXRS that has the time resolution up to 2 ms. Figure 7 shows an example discharge where the magnetic braking due to the RWM occurred. On this discharge, the RWM was triggered by an ELM and then the RWM was growing with the resistive wall time τ_w . Note

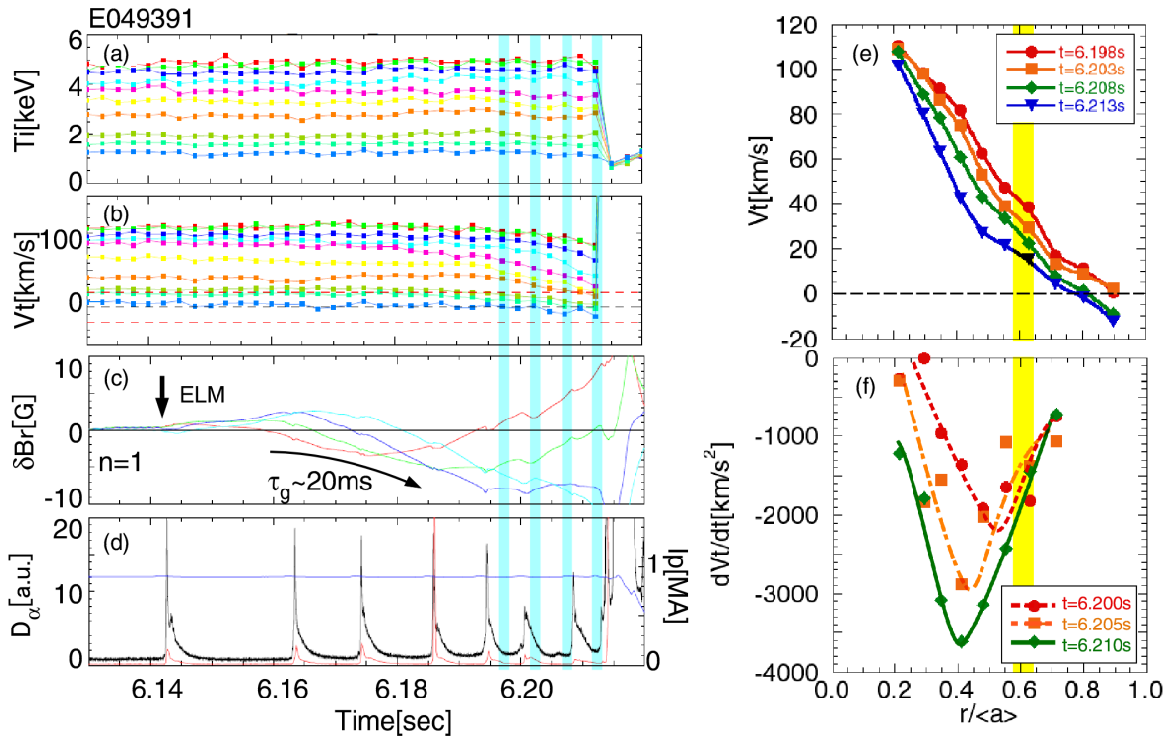


Fig. 7: Waveforms of example discharge where the RWM magnetic braking was observed: Temporal evolutions of (a) ion temperatures, (b) toroidal rotations, (c) $n = 1$ magnetic deviation and (d) D_α emission. Profiles during magnetic braking: (e) toroidal rotation and (f) toroidal acceleration.

that the growth time on this discharge is a factor 2 larger than τ_w . Finally, the radial magnetic amplitude was reached to 10 Gauss at the wall. Figure 7(a) and (b) show the time evolution of the ion temperature and the toroidal rotation. The rotation was gradually decreasing as the RWM growing for 30 ms, while the ion temperature was almost constant.

Figure 7(e) and (f) show the changes of the rotation and the acceleration dV_t/dt profiles during the RWM growing. The plasma rotation began to be globally decelerated due to the RWM. In particular, the plasma rotation inside $q = 2$ surface was mainly reduced as the RWM amplitude increases. As shown in Fig. 7(f), the acceleration profiles, where the minus sign means deceleration, initially have a peak just inside the $q = 2$ surface. As the RWM was growing, the deceleration peak moved from there to further inside region. Note that since the torque input by NBs was kept constant during the RWM growing, the drag estimated from the time derivative of the rotation profile dV_t/dt is valid. Ac-

According to the MARG2D code, on this discharge the $n = 1$ kink-ballooning mode is unstable with no-wall. Figure 8 shows the radial displacements as eigen-function of this unstable mode. This eigen-function has the dominant $m = 2$ component, of which amplitude peak is just inside the $q = 2$ surface. It should be noted that the qualitative estimation by using the ideal MHD stability analysis is valid despite the observed mode is the RWM. The observed results show that the radial mode structure can decide the location where the drag force affect.

5. Summary

The dynamics and stability of the RWM are investigated in the JT-60U high- β plasmas, and the sustainment of high- β_N plasmas above $\beta_N^{\text{no-wall}}$ has been demonstrated using a plasma rotation. We have successfully sustained $\beta_N \simeq 3.0$ for ~ 1 s or $\beta_N \simeq 2.8$ for ~ 5 s by the plasma rotation. In the high- β_N plasmas, some MHD instabilities that can induce the disruption have been observed. In particular, $n = 1$ bursting mode and slowly growing mode as a RWM precursor have been observed at $\beta_N > \beta_N^{\text{no-wall}}$. The bursting mode, which has the growth and decay time with similar τ_w , can sometimes trigger the RWM or change to the slowly growing mode. The observed results show that the bursting mode is thought to be the results the results of a kinetic contribution of energetic particles to the RWM. The slowly growing mode, which has a longer growth time than τ_w and but does not has any islands around rational surfaces, can induce the rotational shear damping. The trajectories between V_t and dV_t/dr shows that both the rotational shear is also important as well as the rotation speed V_t . When the rotational shear was close to zero, the RWM was destabilized despite the enough rotation speed for the RWM stabilization. This result suggests that the rotational shear around the rational surface is important to determine the RWM stability as well as the rotation speed. Moreover, the plasma

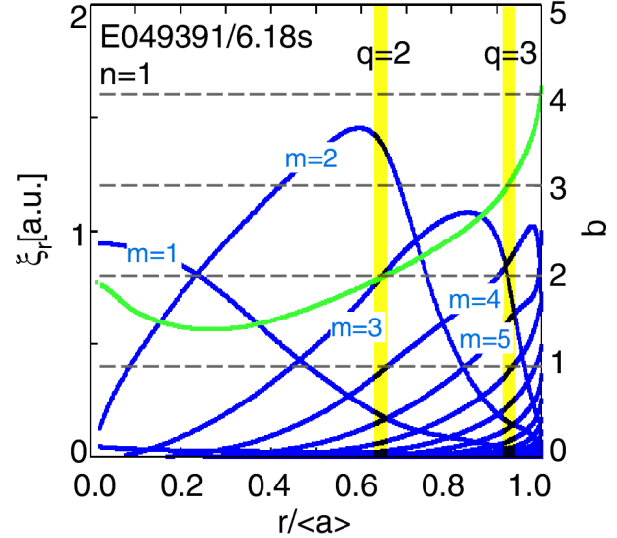


Fig. 8: $n = 1$ radial displacements as eigen-function with no-wall by MARG2D and q -profile by MSE measurement.

rotation braking owing to the RWM have been observed. It is found that the RWM distortion can clearly induce the plasma rotation braking inside the $q = 2$ surface. These results show that the dynamics relating the RWM has a large variety and the RWM stability thought to be determined by not only the plasma rotation but also the kinetic effect and rotational shear.

References

- [1] A. Bondeson and D. J. Ward, Phys. Rev. Lett. **72**, p.2709 (1994).
- [2] M. Takechi et al., Phys. Rev. Lett. **98**, p.055002 (2007).
- [3] H. Reimerdes et al., Phys. Rev. Lett. **98**, p.055001 (2007).
- [4] S. Tokuda and T. Watanabe, Phys. Plasmas **6**, p.3012 (1999)
- [5] Bo Hu and R. Betti, Phys. Rev. Lett. **93**, p.105002 (2004).